Controlling β-Sheet Assembly in Genetically Engineered Silk by Enzymatic Phosphorylation/Dephosphorylation[†]

S. Winkler, D. Wilson, and D. L. Kaplan*

Department of Chemical and Biological Engineering and Bioengineering Center, Tufts University, 4 Colby Street, Medford, Massachusetts 02155

Received June 12, 2000; Revised Manuscript Received August 8, 2000

ABSTRACT: Enzymatic phosphorylation and dephosphorylation reactions were used to modify a genetically engineered variant of spider dragline silk. The ~25 kDa protein was phosphorylated with cyclic AMP-dependent kinase and dephosphorylated with calf intestinal alkaline phosphatase. Phosphorylation inhibited β-sheet assembly of the protein and enhanced solubility to about 5 mg/mL in water, compared to about 20% of this level upon enzymatic dephosphorylation. The cyclability of the phosphorylation−dephosphorylation system was confirmed by MALDI with a model peptide. Kinetic studies conducted with [γ-^{32}P]ATP illustrate that the phosphorylation reaction proceeds over 6 h. Secondary structure of the phosphorylated and dephosphorylated proteins was determined by CD and FTIR. The results illustrate that an enzymatic phosphorylation event can be used to control the solution structure of a protein like silk, which has a tendency to prematurely precipitate due to the formation of β-sheets.

Protein phosphorylation is responsible for the regulation of numerous cell responses and pathways. Besides this regulatory function, phosphorylation can also alter structural features of proteins due to the charge and bulkiness of the phosphate group. For example, enzymatic phosphorylation has been employed to control the inverse temperature transition of elastin (*1*).

Interest in self-assembly of fibrous proteins in novel biomaterials has led to the generation of recombinant silk-like fibrous proteins. A significant limitation in these studies has been the difficulty in maintaining the solubility of the purified genetically engineered silk-like proteins. Premature precipitation arises due to β-sheet formation. This precipitation process is problematic since it is extremely difficult to resolubilize the protein for subsequent characterization of solution structure and properties, or for the fabrication of materials such as membranes or fibers (*2*). Thus, a need exists to gain control of the β-sheet assembly process so that high concentrations of silk proteins can be maintained in aqueous solution in order to study assembly and subsequent formation of fibers and other materials during the processing of native or genetically engineered silks. Furthermore, this control of solubility will lead to options to emulate the natural silk spinning process wherein high concentrations (~30%, w/v) of protein are maintained in an aqueous soluble state prior to being spun into water-insoluble fibers (*3*−*5*).

Synthetic dragline silk-like encoding genes were designed (*6*, *7*) to incorporate a recognition site (RGYSLG) for cyclic AMP-dependent kinase (PKA)[1] in the vicinity of the β-sheet-forming domain. The serine/threonine kinase PKA phosphorylates motifs of the type RXS* and RXXS* (*8*). The phosphorylation motif RGYS*L has been shown to be a high-affinity site for PKA (*9*) and was included in the consensus sequence of the recombinant silk based on minimal change of the core consensus native dragline silk sequence.

The objective of the present study was to employ enzymatic phosphorylation/dephosphorylation to regulate the assembly of the β-sheet secondary structure in silk-like proteins. The polyalanine hydrophobic domain interactions lead to β-sheet formation (*10*). In the phosphorylated state, the protein alcohol group of the serine is modified to a phosphate ester. The expectation is that the formation of the β-sheet would be inhibited (or impaired) by the added phosphate group due to a combination of increased bulkiness and charge−charge repulsion. The prevention of intra- or interchain β-sheet structures should improve the solubility of the protein. The phosphorylation 'trigger' is activated by dephosphorylation using calf intestinal alkaline phosphatase (CIP) (*11*). Upon dephosphorylation, the silk-like proteins are expected to readily form β-sheets leading to reduced solubility. To evaluate the phosphorylation trigger, a ~25 kDa silk-like protein was genetically engineered, expressed in *Escherichia coli*, and characterized in the unphosphorylated and phosphorylated states by SDS−PAGE, CD, and FTIR, and for solubility. Two peptide analogues of this protein were synthesized for more detailed biochemical studies, including MALDI to assess the reversibility and stability and the reaction kinetics of the trigger system. The results show that the enzymatic 'trigger' can be used to influence the solution behavior of β-sheet-forming proteins such as silks.

[†] Supported by the National Science Foundation, Division of Materials Research (Grant DMR-9708062), and the W. M. Keck Foundation for the Biomimetic Materials Characterization Laboratory.

* Corresponding author. Phone: 617-627-3251, E-mail: david.kaplan@tufts.edu.

[1] Abbreviations: PKA, cyclic AMP-dependent kinase; CIP, calf intestinal alkaline phosphatase; IPTG, isopropyl-β-D-thiogalactoside; CD, circular dichroism; FTIR, Fourier transform infrared spectrophotometry; MALDI-MS, matrix-assisted laser desorption ionization mass spectrometry.

10.1021/bi001335w CCC: $19.00
Published on Web 09/21/2000

MATERIALS AND METHODS

Shuttle Vectors pUC·link and pCR·link. A synthetic adapter was ligated into the *Xba*I site of pUC18, forming the *ampicillin*-resistant shuttle vector pUC·link, following the protocol of Prince et al. (*6*). A similar approach was used to create a *chloramphenicol*-resistant shuttle vector, pCR·link. The vector pCR script (Stratagene, Cambridge, MA) was blunt-end-ligated, digested with *Bam*HI, and dephosphorylated using CIP. The linker oligonucleotides were cut with *Bam*HI and ligated into pCR.

Gene Construction. One oligonucleotide monomer building block was 99 nucleotides long and encoded a protein of 2608 Da [SG**RGYS*LG**GQGAGAAAAAGGAGQGGYGGLGSQG]. The polyalanine β-sheet-forming domain is underlined, and the cAPK recognition site is in boldface, with the phosphorylation site marked by (*). The synthetic silk monomer was cloned into the *Nhe*I/*Spe*I sites of either pUC·link or pCR·link using the following method. The plasmid was purified from an overnight cell culture by using a slightly modified method of Birnboim and Doly (*12*). Plasmid DNA was double-digested with *Nhe*I/*Spe*I and dephosphorylated using CIP. The annealed silk monomer was ligated into the vector with T4-Ligase. The reaction mix was then used to transform competent *E. coli* strain BLR(DE3), using the method of Hanahan (*13*). Transformants were identified by incubation on an LB-plate containing the appropriate antibiotic (chloramphenicol for pCR·link, and ampicillin for pUC·link). Recombinant plasmids were screened for insertion of the silk gene monomer by digestion with *Bam*HI and subsequent electrophoresis on 2% agarose gels. Inserts cloned in the correct orientation could be excised from the plasmid by double digestion with *Nhe*I/*Spe*I.

Higher order multimers were constructed by first cloning the monomer into the second shuttle vector using *Bam*HI. In the second step, one plasmid containing the monomer was double-digested with *Nhe*I/*Spe*I. The other monomer containing plasmid (referred to as recipient) was digested with *Spe*I and then treated with CIP. Both digests were phenol-extracted, mixed together, ligated, and transformed into *E. coli*. Transformants were selected based on the antibiotic resistance of the recipient plasmid. Plasmids isolated from the transformants were screened for dimers by digestion with *Bam*HI. Dimer-containing plasmids were double-digested with *Nhe*I/*Spe*I to screen for direct insertion. The new higher order multimer was then cloned again into the *Bam*HI site of the empty second shuttle vector, and the process was repeated.

Expression. The silk gene construct was cloned into the *Bam*HI site of the expression vector pET30a (Novagen). The expression system, pET30a(+) (5422bp), contains an N-terminal His·Tag/thrombin and S·Tag/enterokinase configuration for production of a fusion protein. The His·Tag was used for purification, the S·Tag to quantify the unpurified fusion protein. Enterokinase was used to cleave the Tags according to the manufacturers' procedures.

Escherichia coli strain BLR(DE3) [F^- *ompT hsdS*$_B$ (r_B^- m_B^-) *gal dcm* Δ(*srl-recA*)306::Tn10 (DE3)] (Novagen, Madison, WI) was used as a host for cloning and expression and grown under aerobic conditions at 37 °C in a 10 L fermenter (New Brunswick Scientific) using supplemented complex media containing (in g/L) 5 glucose, 5 yeast extract, 1.7 citric acid, 4 $(NH_4)_2HPO_4$, 13.3 KH_2PO_4, 1.2 $MgSO_4$, 0.1 $FeSO_4$, 0.02 $CaCl_2$, 0.02 $ZnSO_4$, 0.01 $CuSO_4$, 0.005 $MnSO_4$, 0.001 $(NH_4)_6Mo_7O_{24}$, 0.0002 $Na_2B_4O_7$ (*14*). A feeding solution of 500 g/L glucose, 250 g/L yeast extract, and 20 g/L $MgSO_4$ was added during the growth and induction period based on the uptake rate and dissolved oxygen readings. Pure oxygen was used to supplement the air fed to maintain the DO level over 10%. Protein synthesis was induced with isopropyl-β-D-thiogalactoside (IPTG) at a final concentration of 1 mM. The cultures were harvested and centrifuged at 4 °C, 6000*g*, for 10 min. The pellet was resuspended in a volume 3 times its weight of purification buffer (300 mM NaCl, 50 mM NaH_2PO_4, 5 mM imidazole, pH 8) containing Mini Complete Protease Inhibitor (Boehringer Mannheim) and subsequently put through a cell homogenizer at 10 000 psi. The lysate was centrifuged at low speed (4 °C, 4000*g*, for 30 min) to remove unlysed cells, and the supernatant was then centrifuged at 4 °C, 10000*g*, for 120 min to remove remaining cell debris. The supernatant containing the unpurified protein was stored at −70 °C until further processing.

The recombinant silk protein was purified by Ni-chelate chromatography (Qiagen), washed extensively with 50 mM imidazole, and eluted using 250 mM imidazole. Purified proteins were dialyzed using Snake Skin dialysis tubing (MWCO = 10 000) (Pierce) against water to remove salts and then lyophilized.

Peptide Synthesis. Peptide synthesis was carried out by the Tufts Protein Core Facility on an Applied Biosystems Peptide-Synthesizer. Peptides were subsequently purified using RP-HPLC. Two peptides containing a PKA phoshorylation site within the core repeat and with and without the polyalanine crystalline repeat, $(E)_5$SGRGYSLGGQAG$(A)_5$GGAGQYGGLGSQG$(E)_5$ (PHOS1) and $(E)_5$SGRGYSLGGQAGAGGAGQYGGLGSQG$(E)_5$ (PHOS2), were prepared, with solubilizing blocks $(E)_5$ at each terminus.

Phosphorylation Reactions. Purified protein was phosphorylated by incubating approximately 1 mM protein in phosphorylation buffer (50 mM TRIS or 50 mM cacodylic acid, 10 mM $MgCl_2$, pH 7.5) with 5 units of cAPK and 20 mM ATP at 30 °C for various amounts of time. For the labeling reactions, 10 mM ATP was substituted with [γ-^{32}P]-ATP. Removal of the phosphate groups was achieved by incubating the phosphoryated protein with CIP in identical buffer conditions at 37 °C for various amounts of time. For structural analysis, removal of the enzymes was achieved from the phosphorylation/dephosphorylation reaction either by repurifying the protein using the His·Tag of the silk protein or by using Sephadex gel-filtration columns. The buffers were exchanged against water using dialysis prior to structural analysis.

Autoradiography. Labeled protein was run on SDS−PAGE, and the gel was washed to remove any unbound [γ-^{32}P]ATP and dried. The dried gel was exposed to X-ray film (Kodak) at −70 °C overnight and the film developed using standard procedures. For labeling reactions, Kemptide (*15*) (LARRAS*VA) (Sigma) was used as a positive control; a recombinant silk lacking the cAPK recognition site was used as a negative control.

Phosphotransfer. Kinetic studies of protein kinase activity toward silk were performed using a phosphocellulose filter binding assay (*16*, *17*). Phosphotransfer to the serine residue

of the silk protein or the peptides was measured by reaction of PKA with the silk protein in the presence of [γ-^{32}P]ATP. Trichloroacetic acid (24% w/v) is added to stop the reaction, and the silk, which upon phosphorylation is positively charged, was spotted onto Whatman P81 chomatography paper circles. The chromatography paper circles were washed 4 times in 500 mL of phosphoric acid (75 mM) and finally briefly rinsed in 80% ethanol. The radioactivity incorporated into the target protein was quantified using a liquid scintillation counter. Kemptide was used as a positive control, a reaction with the recombinant silk but lacking the PKA was used as a negative control, and a chromatography paper square was subjected to the resolution of 4 and a 1000 μm spot. To prevent charging of the sample surface, a nickel wire mesh was positioned ~5 mm above the sample, and a flood gun was used at 5 eV. Peak areas were measured using the ESCA software supplied with the instrument.

Solubility Measurements. Samples of lyophilized protein in both phosphorylated and unphosphorylated states were resolubilized with water so that a supersaturated solution resulted (i.e., precipitate was visible). Samples of known volume (1 mL) of the supernatant were taken and lyophilized, and the dry protein was weighed to estimate the solubility of the silk proteins. The same volume of each solution was also run by SDS−PAGE.

MALDI-TOF. A Perkin-Elmer Voyager mass spectrometer (Protein Core Facility, Tufts Medical School) was used for molecular weight determinations. A solution of 1 μg/μL protein or peptide was mixed with a 10^4-fold molar excess of the matrix in an aqueous 30% acetonitrile solution containing 0.1% trifluoroacetic acid. Sinapinic acid was used as the matrix with the recombinant protein and 2,5-dihydroxybenzoic acid for the peptide.

Fourier Transform Infrared Spectroscopy. Infrared spectroscopy data were gathered in both the solid and solution states utilizing FTIR microscopy and an attenuated total reflectance (ATR) cell (Bruker Equinox 55; Billerica, MA) at 4 cm^{-1} resolution. Solid-state spectra were taken for dried peptides dropped from an 1−1.6 mg/mL aqueous solution onto a ZnS crystal. Solution-state characterization was carried out with peptide solutions placed in a ZnSe ATR crystal cell. Spectra were taken from ~1 mg/mL aqueous solutions of the peptides at 35 reflections per measurement. ATR-FTIR experiments required lower concentrations in order to avoid overloading the ATR cell. Spectra were also taken after solvent evaporation.

The amide I band curves were fitted using Peak Fit v4 (SPSS Science Software Products) residual peak detection and fitting procedure. Baseline determination was accomplished by a linear regression analysis, data smoothing utilized the Savitsky−Golay smoothing function, and Voigt amplitude function was used to curve-fit data peaks (*18*, *19*). The Voigt amplitude function convolves a "natural" Lorentzian waveform and an independent Gaussian instrument broadening, thus producing a theoretical model for spectral lines when both types of expansion are present. The contribution of each curve to the amide I band was assessed by integrating the area under the curve and then normalizing to the total area under the amide I band.

Circular Dichroism. Solution-state circular dichroism spectra were recorded on a Jasco J-710 spectropolarimeter (Easton, MD) between 190 and 240 nm. Protein solutions, of 1 mg/mL, were prepared in Milli-Q (Millipore) ultrapure water and analyzed with a path length of 0.1 cm. Spectra deconvolution was performed using a neural network-based deconvolution program, CDNN.

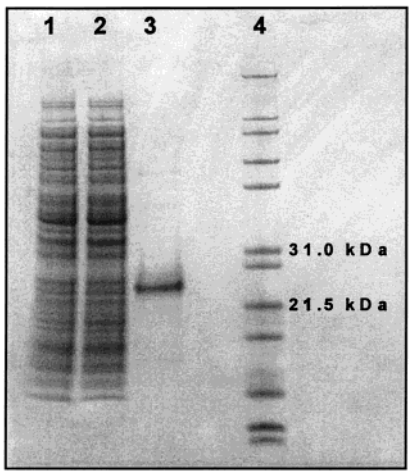

FIGURE 1: SDS−PAGE of recombinant silk fermentation. Lane 1, uninduced whole cell extract; lane 2, 3 h (at harvest) induced whole cell extract; lane 3, purified protein (cleaved); lane 4, molecular mass markers.

RESULTS

Expression and Processing. A genetically engineered silk gene was constructed to encode a protein of ~25 kDa (5 repeats of the monomer sequence). After expression and purification of the pentamer, the protein appeared as a single band running slightly higher than the expected molecular mass of 25 kDa (Figure 1).

Figure 1 shows the uninduced and induced cell extracts and the final purified protein by SDS−PAGE. There was no difference observed in uninduced and induced cell extracts, suggesting that the pentamer is expressed at relatively low levels. Based on analysis of the soluble and insoluble fractions, the product appeared exclusively in the soluble fraction of the cell extract. The yield, determined per liter of cells from the S·Tag assay at an OD_{600} of 1.0, ranged from 25 to 40 mg/L. To overcome the low expression, protein production was carried out in high-density fermentations with induction cell densities of OD_{600} of above 50 and extended induction times. While the productivity per cell during these runs was at the lower level of the spectrum for recombinant silks, final product yields of 16 mg/L of purified protein could be achieved, compensating for the low productivity with high cell densities. This protein was studied in subsequent phosphorylation/dephosphorylation experiments.

Enzymatic Phosphorylation. Phosphorylation/dephosphorylation of the protein was assessed by phosphorylating the recombinant silk with [γ-^{32}P]ATP in the presence of PKA and CIP (Figure 2).

Phosphorylation proceeded immediately, leveling out around 6 h. There is a slight increase in band intensity when incubating for extended periods of time (24 h). The same experiment using a recombinant silk, lacking the phosphorylation site, yielded no signal. This indicates that the serine phosphorylated is in fact the serine in the phosphorylation site and not other serines in the tags or protein sequence.

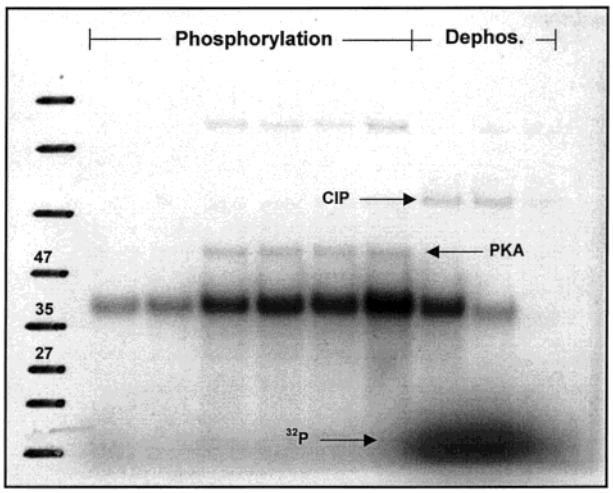

FIGURE 2: Autoradiography of silk phosphorylation. Phosphorylation after 30 min, 1 h, 2 h, 6 h, 12 h, and 24 h. Dephosphorylation of the 24 h sample at 1, 6, and 24 h. Weight markers were marked on the X-ray film by hand.

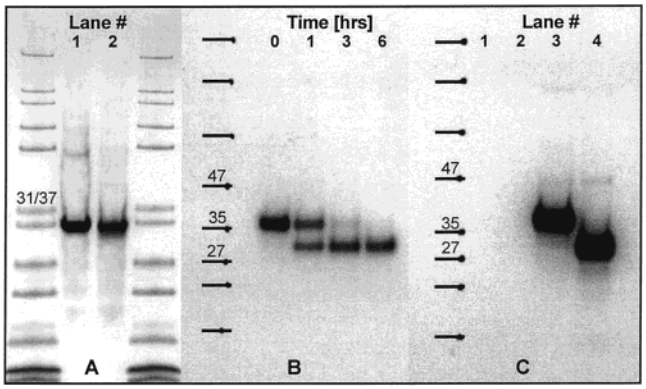

FIGURE 3: SDS−PAGE and autoradiography pictures of silks. (A) SDS−PAGE of phosphorylated (lane 1) and unphosphorylated (lane 2) silk. (B) Autoradiography of enzymatic (enterokinase) cleavage of labeled silk over time. (C) Phosphorylation assay for various reaction conditions. Lane 1, 24 h labeling reaction lacking the kinase; lane 2, 24 h labeling reaction with phosphorylated silk; lane 3, 24 h labeling reaction with unphosphorylated silk; lane 4, 24 h labeling reaction with cleaved unphosphorylated silk.

Dephosphorylation of the 24 h sample showed complete removal of the ^{32}P from the protein in 24 h, demonstrating the reversibility of the reaction. The released free ^{32}P after treatment with CIP gives a signal at the bottom of the gel (Figure 2). The upward band shift of the phosphorylated protein in these gels can be partly explained by the fact that the molecular weight standards are transferred to the X-ray pictures by hand. While some upshift occurs after prolonged storage of the protein and is most likely due to internal structural changes, no shift can be detected due to phosphorylation (Figure 3A).

Phosphorylation of the silk protein does also not hinder the cleavage of the fusion protein by enterokinase (Figure 3B). Furthermore, it can be seen that the radioactivity is retained in the core silk protein, rather than with the fusion tags. Densitometry analysis of the autoradiography picture shown in Figure 3B accounts for more than 90% of the final band intensity compared to the starting material. This result is corroborated by Figure 3C. Phosphorylation of identical amounts of cleaved and uncleaved silk protein for 24 h yields almost identical band intensities. Cold-ATP phosphorylated

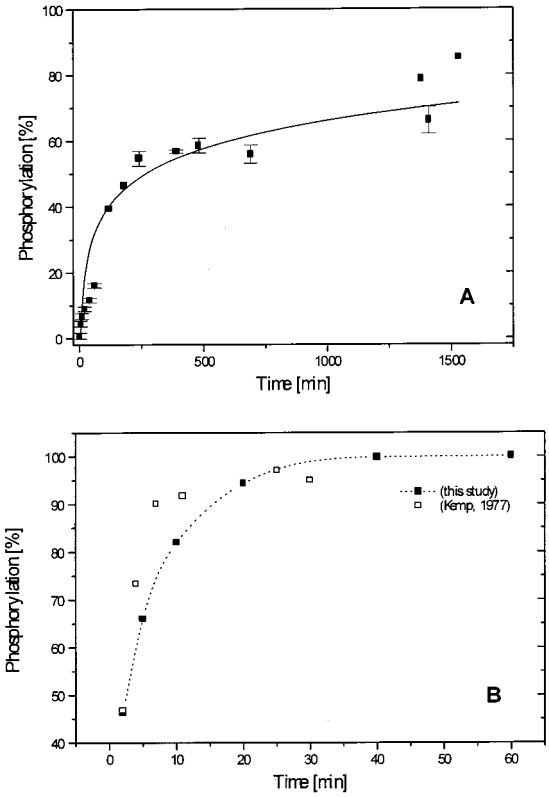

FIGURE 4: (A) ^{32}P transfer to the recombinant silk protein determined by liquid scintillation. (B) ^{32}P transfer to Kemptide determined by liquid scintillation. For comparison, data from Kemp et al. (*15*) are included as open squares.

Table 1: Average CD Interpretations of the Unphosphorylated and Phosphorylated Silk Proteins, along with a Comparison to Native Spider Dragline Silk (from FTIR)

sample	β-strand (%)	silk I or random coil (%)
native spider dragline silk (*21*)	31	15
silk protein (unphosphorylated)	52 ± 3	26 ± 2
silk protein (phosphorylated)	43 ± 2	34 ± 2

silk and a labeling reaction without the PKA show no signal, indicating that no nonspecific phosphorylation takes place and that the phosphorylation is stable.

Phosphorylation of the silk protein proceeds in an exponential (first order) fashion, leveling at about 60% of the theoretical complete phosphorylation of all sites (Figure 4A). This is supported by elemental analysis with XPS indicating 60−73% phosphorylation. Compared to the high-affinity substrate Kemptide (Figure 4B), the phosphotransfer is about 24 times slower based on $v_{max}/2$. The results of the kinetic experiments are in accordance with the autoradiography studies, which show the reaction of 1 mM recombinant silk substrate with 5 units of PKA leveling out around 6 h. The incomplete phosphorylation of the silk likely indicates that complete access to the phosphorylation sites is hindered. This suggests that some silk secondary structure is present. This possibility is corroborated by the CD/FTIR data (Tables1 and 2) that show residual β-sheet in the triggered phosphorylated state. Phosphorylation of the monomeric peptides showed the same kinetic behavior as for the silks; however, complete phosphorylation was achieved.

Conformational Studies in Solution: CD. Unphosphorylated and phosphorylated samples of the protein were

Table 2: Average FTIR Interpretations of the Unphosphorylated and Phosphorylated Silk Proteins, along with a Comparison to Native Spider Dragline Silk

sample	β-strand (%)	silk I or random coil (%)
native spider dragline silk (*21*)	31	15
silk protein (unphosphorylated)	51 ± 4	14 ± 3
silk protein (phosphorylated)	34 ± 8	17 ± 4

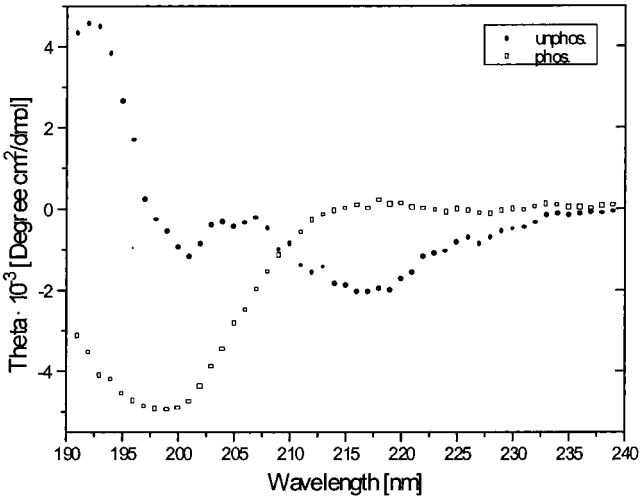

FIGURE 5: CD spectra for unphosphorylated and phosphorylated silk.

characterized by CD. Approximately 1.6 mg/mL protein in ultrapure water was characterized. For both forms, the amounts of α-helix and β-turn were comparable and remained more or less constant. The structural changes induced by the trigger decreased the β-sheet content and increased the random coil content (Figure 5). The phosphorylated sample had lower absorption at 216 nm (β-pleated sheet) and a higher absorbance in the 200 nm range (random coil). By deconvoluting several spectra, it was possible to quantify the structural transition (Table 1). The unphosphorylated form of the protein contained a higher percentage of β-sheet than the phosphorylated protein (52% versus 43%) and a lower content of random coil (26% versus 34%). No significant change in conformation was observed when the fusion Tag was cleaved off.

Conformational Studies in Solution: FTIR. Solution-state conformational data were obtained using ATR-FTIR. In the initial stages of the experiment, all silk protein was in solution, but in contact with or near the crystal. Over the course of the measurements, little silk protein adsorbed onto the hydrophobic surface of the ATR cell crystal, and a protein layer formed only after the solution was left on the cell long enough to evaporate.

Solutions of the proteins were also dried on ZnS crystals for FTIR analysis. In protein adsorption studies, strong conformational changes are generally associated with adsorption to highly hydrophobic surfaces from aqueous solution, while hydrophilic and mildly hydrophobic surfaces, such as ZnS, preserve the solution-state conformation. FTIR spectra of dried films include both the dried solution and small particulates that may have been suspended in solution. No difference in the spectra obtained was observed either, over time in the solution studies, while the protein layer formed, or in the dried films. When qualitatively comparing IR

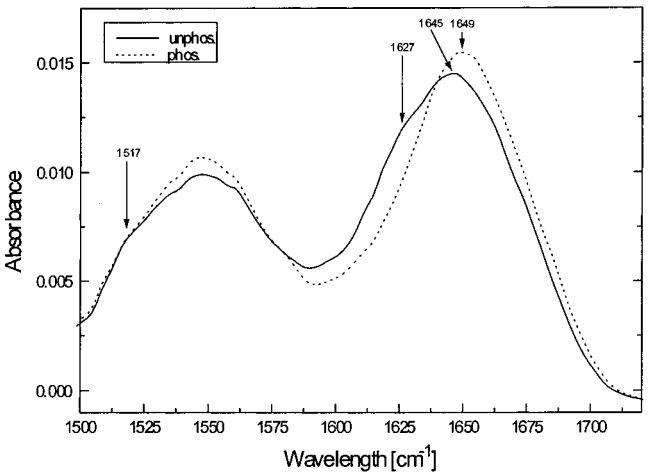

FIGURE 6: FTIR spectra of the amide I and amide II regions for unphosphorylated and phosphorylated silk.

spectra of unphosphorylated and phosphorylated silk solutions (Figure 6) with similar amounts of protein, as seen from the similar intensity of the tyrosine absorption at 1517 cm^{-1}, the following trends were observed. Upon phosphorylation, the protein structure changes, and the unphosphorylated protein loses a significant amount of β-structure since the peak at 1627 cm^{-1} almost disappears. The amide I peak shifts from 1645 (β-structure) to 1649 cm^{-1} (random or helical), showing the loss of β-associated structure (*20*). Deconvolution of several spectra supports the significant difference between the unphosphorylated and phosphorylated samples, with a higher proportion of β-strand and random coil in the unphosphorylated and phosphorylated forms, respectively (Table 2).

MALDI of Proteins and Model Peptides. The recombinant silk proteins, both as expressed and phosphorylated, failed to give a signal in the MALDI analysis. This failure is most likely due to the structure and highly hydrophobic behavior of those proteins, preventing ionization at energy levels below the decomposition threshold, and has been experienced with other genetically engineered silks and silk-like proteins. The model peptide monomers, however, with calculated masses of 3846 Da (PHOS1) and 3377 Da (PHOS2), were confirmed by MALDI. Overnight incubation of the peptides with PKA initially yielded a mass change of 102 Da for all phosphorylation experiments, which is 25 Da more than expected. This additional mass could either be due to the formation of a Mg^{2+} salt, since a high concentration of $MgCl_2$ is present in the phosphorylation reaction, or be due to the phosphopeptide flying as a Na adduct (22 Da increase) during MALDI-MS. Stripping metal ions using an additional incubation with EDTA yielded a 77 Da mass gain consistent with the phosphorylation of one serine (Figures7 and 8A) per peptide.

The phosphorylated samples were analyzed after 1 week storage at room temperature and exhibited no sign of degradation (i.e., no change in the expected molecular weight), showing that the phosphorylated states of the modified peptides were stable. Upon incubation of these samples with CIP, the original weight was restored, showing the peptides could be dephosphorylated to cycle back to the initial state (e.g., completing the full cycle of the trigger), based on the reappearance of the peaks at 3847 (±2) and

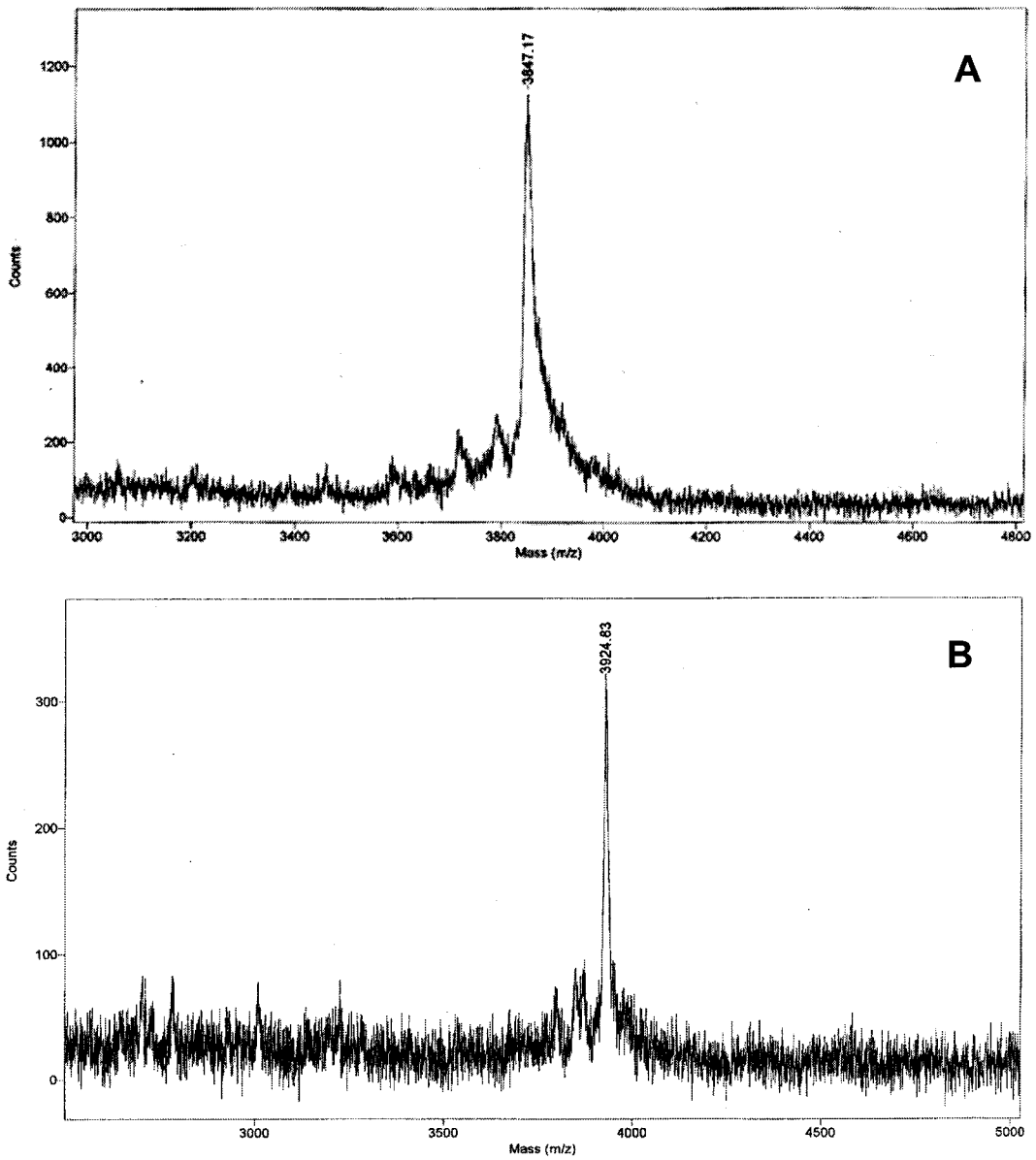

FIGURE 7: MALDI analysis of the peptide analogue PHOS1. (A) Unphosphorylated form. (B) Phosphorylated form after incubation with PKA.

3479 (±2) Da (Figure 8). This demonstrates that the modification achieved was in fact an enzymatic phosphorylation and that the alcohol group in the serine side chain was successfully modified by phosphorylation.

Solubility. The unphosphorylated silk protein was soluble in H_2O at ~1.6 mg/mL immediately after the purification process and before lyophilization. After lyophilization or prolonged storage (weeks) in solution, the protein solubility decreased to about 0.9−1.3 mg/mL at room temperature in H_2O. The phosphorylated silk could be rehydrated to a concentration of 5−6 mg/mL in H_2O and readily went into solution. The significant difference in solubility is shown in Figure 9. Equal volumes of saturated protein solutions, unphosphorylated and phosphorylated, respectively, show different band intensities. Densitometric analysis of the gel indicates that about 5 times more protein is present in the band for the phosphorylated silk. While lyophilization and storage effects were observed with the phosphorylated silk, they were much less dominant than in the untriggered state. These results indicate that the hydrophobic interactions of the β-sheets, which reduce solubility, are less dominant in the phosphorylated state and solubility can be regulated by controlling β-sheet formation by enzymatic phosphorylation.

DISCUSSION

β-Sheet-forming proteins are notoriously difficult to maintain in aqueous solution due to the presence of hydrophobic crystals that exclude water and render the protein insoluble. This problem occurs especially in reprocessed silk proteins or genetically engineered variants of these proteins. High concentrations of lithium bromide or lithium thiocyanate are often required to reduce the hydrogen bonding to promote solubility, since traditional solvents and chaotropic agents are completely ineffective (*2*, *22*). However, spider dragline silk resists even these treatments in comparison to silkworm silk (*2*).

In natural silk processing and silk fiber spinning, the solubility problem has been overcome by mechanisms that are not fully understood. Both spiders and silkworms are

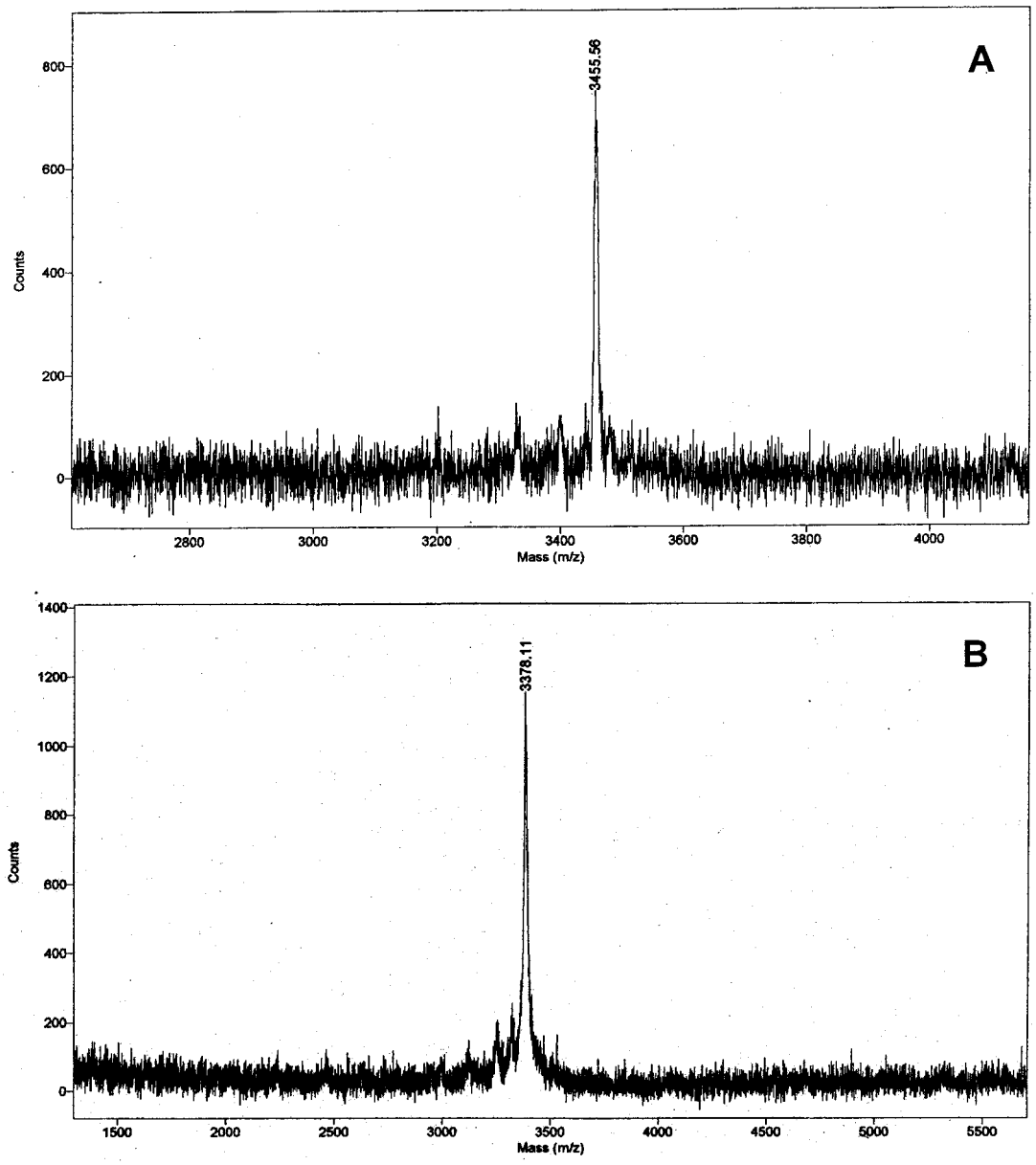

FIGURE 8: MALDI analysis of the peptide analogue PHOS2. (A) Phosphorylated form. (B) Dephosphorylated form after incubation with CIP (from phosphorylated sample shown in Figure 5A).

able to maintain relatively high concentrations (~30 wt %) of solubilized silk in storage prior to spinning. The presence of liquid-crystalline phases formed through self-assembly processes may play a critical role in this process (*23*, *24*). In addition, different conformations of the silk in solution have been characterized. In particular, the metastable silk I form(s) seem(s) to be important to maintain solution behavior in storage (*24*).

The transition process from soluble silk protein polymer chains secreted into the lumen of the storage glands, to the final spun and now water-insoluble silk fibers, provides a useful system with which to gain insight into β-sheet assembly. The transition is mostly due to physical shear (*25*, *26*), and the process proceeds without obvious posttranslational chemical modifications except for the possible involvement of a single disulfide oxidation−reduction step in the silkworm fibroin assembly (*27*), which might also be the case in spider silk (*28*). So far no kinase involvement in the silk assembly process has been reported; however, it is known that salts, which are a necessary factor of kinase activity, play a role in the control of solubility and of the structural transition from silk I to silk II (*25*, *29*).

To gain insight into this assembly process, an enzymatic trigger system was designed and studied. The assumption in the design was that the insertion of a phosphorylation site would be a sufficiently small modification to avoid disrupting the normal silk assembly processes. The phosphorylation of the protein did cause a decrease in the β-structure content of the protein, but did not completely inhibit the β-sheet assembly process. The enzymatic modifications carried out with the model peptides also illustrated that the process was stable and reversible. While the phosphorylation of the Kemptide proceeded completely with values comparable to the literature, phosphorylation of the silk protein modified about 60% of the possible sites, although slightly higher phosphorylation was observed occasionally. This incomplete phosphorylation might be due to residual secondary β-structure, as indicated by FTIR and CD analysis, which may

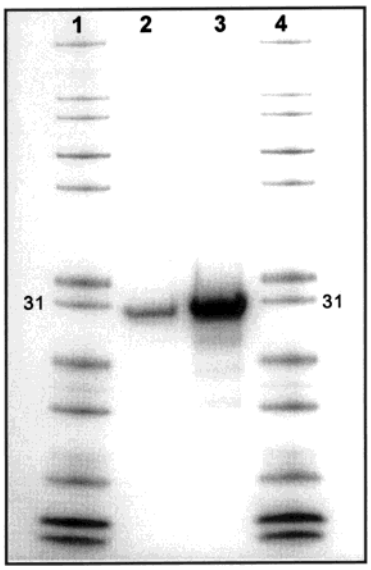

FIGURE 9: SDS−PAGE of equal volumes of saturated silk solutions. Lanes 1 and 4, molecular weight markers; lane 2, unphosphorylated silk; lane 3, phosphorylated silk.

prevent access of the enzyme to all of the phosphorylation sites. The overall solubility of the phosphorylated protein was increased about 4-fold compared to the unphosphorylated form. Therefore, even with the apparent incomplete phosphorylation, the enzymatic phosphorylation triggering system appears to function as designed and offers an additional option in modulation of assembly processes associated with this type of protein.

The process outlined here may be a useful model to consider in studies of β-sheet assembly in general, including β-amyloid and prion systems, to supplement or in certain cases replace the reduction−oxidation control (*30*). The use of an enzymatic system rather than subjecting the target substrate to harsh chemical conditions provides options for in vitro and in vivo assays to understand the folding and assembly pathways for β-sheet proteins, as well as for other groups of proteins with similar secondary structures. Enzymatic phosphorylation systems in vivo can also provide a window into opportunities to disrupt the β-sheet assembly processes in cases where this is desirable even before proteins are purified.

ACKNOWLEDGMENT

We thank Hagan Bayley for helpful discussions and Lars Waldmann for assistance with the CD analysis.

REFERENCES

1. Pattanaik, A., Gowda, D. C., and Urry D. W. (1991) *Biochem. Biophys. Res. Commun. 178*, 539−545.
2. Mello, C. M., Senecal, K., Yeung, B., Vouros, P., and Kaplan, D. L. (1994) in *Silk Polymers* (Kaplan, D. L., Adams, W. W., Farmer, B., and Viney, C., Eds.) pp 67−69, *Am. Chem. Soc. Symp. Ser. 544*.
3. Kaplan, D. L., Fossey, S., Mello, C. M., Arcidiacono, S., Senecal, K., Muller, W., Stockwell, S., Beckwitt, R., Viney, C., and Kerkam, K. (1992a) Biosynthesis and processing of silk proteins. *Mater. Res. Soc. Bull. 10*, 41−47.
4. Kaplan, D. L., Fossey, S., Viney, C., and Muller, W. (1992b) in *Hierarchically Structured Materials* (Aksay, I. A., Baer, E., Sarikaya, M., and Tirrel, D. A., Eds.) Materials Research Society, Pittsburgh, PA, pp 19−29.
5. Kaplan, D. L., Mello, C. M., Arcidiacono, S., Fossey, S., Senecal, K., and Muller, W. (1998) in *Protein-Based Materials* (McGrath, K., and Kaplan, D. L., Eds.) pp 103−131, Birkhauser, Boston.
6. Prince, J. T., McGrath, K. P., DiGirolamo, C. M., and Kaplan, D. L. (1995) *Biochemistry 34*, 10879−10885.
7. Winkler, S., Szela, S., Avtges, P. J., Valluzzi, R., and Kaplan, D. L. (1999) *Int. J. Biol. Macromol. 24*, 265−270.
8. Kemp, B. E., Graves, D. J., Benjamin, E., and Krebs, E. G. (1977) *J. Biol. Chem. 252*, 4888−4894.
9. Maller, J. L., Kemp, B. E., and Krebs, E. G. (1978) *Proc. Natl. Acad. Sci. U.S.A. 75*, 248−251.
10. Simmons, A. H., Michal, C. A., and Jelinski, L. W. (1996) *Science 271*, 84−87.
11. Sambrook, J., Fritsch, E. F., and Maniatis, T., (1986) in *Molecular Cloning*. Cold Spring Harbor Laboratory, Cold Spring Harbor, NY.
12. Birnboim, H. C., and Doly, J. (1979) *Nucleic Acids Res. 7*, 1513−1523.
13. Hanahan, D. (1983) *J. Mol. Biol. 166*, 557−580.
14. Kim Y. C., Kwon, S., Lee, S. Y., and Chang, H. N. (1998) *Biotechnol. Lett. 20*, 799−803.
15. Kemp, B. E., Graves, D. J., Benjamini, E., and Krebs, E. G. (1977) *J. Biol. Chem. 252*, 4888−4894.
16. Bertics, P. J., and Gill, G. N. (1985) *J. Biol. Chem. 260*, 4642−4647.
17. Wedegaertner, P. B., and Gill G. N. (1989) *J. Biol. Chem. 264*, 11346−11353.
18. Langford, J. I. (1978) *J. Appl. Crystallog. 11*, 10−14.
19. Jansson, P. (1984) *Applications in Spectroscopy*, Academic Press, New York.
20. Wilson, D., Valluzzi, R., and Kaplan, D. L. (2000) *Biophys. J. 78*, 2690−2701.
21. Gillespie, D. B., Viney, C., and Yager, P. (1994) in *Silk Polymers* (Kaplan, D. L., Adams, W. W., Farmer, B., and Viney, C., Eds.) pp 155−167, *Am. Chem. Soc. Symp. Ser. 544*.
22. Lock, R. (1993) PCT Patent W093/15244.
23. Kerkam, K. C., Viney, C., Kaplan, D. L., and Lombardi, S. J. (1991) *Nature 349*, 596−598.
24. Willcox, P. J., Gido, S. P., Muller, W., and Kaplan, D. L. (1996) *Macromolecules 29*, 5106−5110.
25. Ilzuka, E. (1985) Silk: an overview. *J. Appl. Polym. Sci. Jpn. 41*, 163−171.
26. Magoshi, J., Magoshi, Y., and Nakamura, S. (1985) *J. Appl. Polym. Sci. 41*, 187−204.
27. Yamaguchi, K., Kikuchi, Y., Takagai, T., Kikuchi, A., Oyama, F., Shimura, K., and Mizuno, S. (1989) *J. Mol. Biol. 210*, 127−139.
28. Beckwitt, R., and Arcidiacono, S. (1994) *J. Biol. Chem. 269*, 6661−6663
29. Tillinghast, E. K., and Townley, M. A. (1994) in *Silk Polymers* (Kaplan, D. L., Adams, W. W., Farmer, B., and Viney, C., Eds.) pp 29−44, *Am. Chem. Soc. Symp. Ser. 544*.
30. Valluzzi, R., Szela, S., Avtges, P., Kirschner, D., and Kaplan, D. L. (1999) *J. Phys. Chem. 103*, 11382−11392.

BI001335W